Biochimica et Biophysica Acta, 1143 (1993) 183–189

BBABIO 43837

Modulation analysis of the electron spin echo signals of in vivo oxidised primary donor ^{14}N chlorophyll centres in bacterial, P870 and P960, and plant Photosystem I, P700, reaction centres

Ian H. Davis [a], Peter Heathcote [b], Dugald J. MacLachlan [a] and Michael C.W. Evans [a]

[a] *Department of Biology, Darwin Building, University College London, London (UK) and* [b] *School of Biological Sciences, Queen Mary and Westfield College, London (UK)*

(Received 17 August 1992)

Key words: Modulation analysis; Electron spin echo; Chlorophyll center; Reaction center; Photosystem I; (Bacteria); (Spinach)

The primary donors of two structurally characterised photosynthetic bacterial reaction centres, $P870^+$ from *Rhodobacter sphaeroides* and $P960^+$ from *Rhodopseudomonas viridis*, and the spinach Photosystem I primary donor $P700^+$ were studied by electron spin echo modulation. The values obtained for the in vivo isotropic hyperfine interaction, a_{iso}, were considerably smaller than literature reports from in vitro studies. The results for $P960^+$ and $P870^+$ are in accord with data from other spectroscopic techniques and reveal that the electron is more localised in one half of the chlorophyll dimer with a ratio of 2:1. Damping of the modulations was most severe for $P960^+$, which interacts with the non-haem iron of the reaction centre as well as a donor cytochrome, cyt *c*. The reduced hyperfine interactions obtained for $P700^+$ indicate that $P700^+$ is either a chlorophyll dimer with the electron extensively localised on one of the chlorophyll pair with a ratio of 3:1 or 4:1, depending on which of the published values of a_{iso} for chlorophyll a^+ is used, or a monomer.

Introduction

The primary photochemical event in photosynthesis is the photooxidation of chlorophyll and transfer of an electron to a chlorin acceptor. The photochemically active chlorophyll is distinguished from the bulk chlorophyll involved in light harvesting and energy transfer by spectral and redox properties. It is well established that in purple photosynthetic bacteria, *Rhodobacter sphaeroides* and *Rhodopseudomonas viridis*, the photochemically active species is a dimer of bacteriochlorophyll molecules in an environment defined by the L and M subunits of the reaction centre. This special pair of reaction centre chlorophylls are not chemically distinct and are not covalently bound to the reaction centre. The special properties of the pair and the mechanism of photooxidation are determined by the protein environment of the reaction centre. The dimeric structure of the reaction centre chlorophyll was originally inferred from the linewidth of the EPR spectrum of the cation in *Rb. sphaeroides*, essentially $\sqrt{2}$ of the linewidth of the bacteriochlorophyll cation in vitro [1], hyperfine coupling constants of the cation determined by ENDOR [2], and the zero field splitting of the spin-polarised triplet formed by the back reaction from the chlorin acceptor to the bacteriochlorophyll donor [3]. This model has subsequently been confirmed by the determination of the crystal structure of the isolated reaction centre [4]. Although the linewidth of the *Rb. sphaeroides* cation EPR spectrum is an excellent fit for a dimer model with the electron delocalised over both chlorophyll molecules this is not the case in *R. viridis*. Subsequent work using ENDOR, both in solution and more recently of single crystals and of mutants in which the special pair is modified as a heterodimer containing one chlorophyll and one pheophytin molecule, indicate that although the dimeric structure is correct the electron distribution is asymmetric. In both bacterial species the electron density is much greater on one of the two chlorophyll molecules than the other [5]. This asymmetry may be of considerable importance in determining the high efficiency of charge transfer and the fact that only one branch of the largely symmetrical reaction centre is used for electron transfer, the initial event being an internal charge separation on the dimer.

Correspondence: M.C.W. Evans, Department of Biology, University College London, Gower St., London, WC1E 6BT, UK.

Abbreviations: ENDOR, electron nuclear double resonance; ESEEM, electron spin echo envelope modulation; P, the photochemically active reaction centre chlorophyll; cyt, cytochrome.

The properties of the reaction centre chlorophylls of plants are less well defined. Plants have two types of reaction centre. Photosystem II, the reaction centre involved in water oxidation is highly analogous to the purple bacterial reaction centre. However, the very oxidising properties of the reaction centre chlorophyll and the instability of purified preparations makes it extremely difficult to investigate spectroscopically. Photosystem I, the reaction centre involved in ferredoxin reduction, is structurally different from the other reaction centres, although the basic photochemical mechanism appears to be essentially the same with photooxidation of a reaction centre chlorophyll (P700) and electron transfer to a chlorin acceptor. Optical studies of this centre are hampered by the large number of light harvesting chlorophyll molecules, at least 40, directly associated with the reaction centre and although crystals have been obtained there is not yet a detailed structure. The structure of P700 is still controversial, there have been a number of suggestions that modified chlorophyll molecules are involved. However, improving isolation procedures suggest that this is in fact unlikely and that as in the bacteria the reaction centre chlorophyll will be a normal chlorophyll molecule in a special environment. It seems likely that P700 will also have a dimeric structure. Optical studies suggest that the ground state of P700 is dimeric [6–8]. The line width of the EPR spectrum is narrowed to $\sqrt{2}$ of the monomer chlorophyll line width as in *Rb. sphaeroides* [9], suggesting a fully delocalised dimer. However, in *Rb. sphaeroides* it is now known that this is misleading, the electron being partly localised on one half of the special pair and the line width modified by local proton coupling. The zero field splitting of the spin-polarised triplet formed by back reaction to P700 is intermediate between that expected for a monomer and a dimer [3]. ENDOR spectra provide support for a dimeric model [10], but have also been interpreted in terms of modified chlorophyll structures or a monomer [11].

ESEEM spectra offer the possibility of determining small hyperfine interactions of the type which occur in chlorophyll cations between the unpaired spin and the nitrogen nuclei of the chlorin ring structure. We have determined the ESEEM spectra of $P700^+$ in natural abundance ^{14}N containing preparations at 4 K and compared these with the spectra of preparations from *Rb. sphaeroides* and *R. viridis*. Analysis of these spectra allows an estimation of the dimeric properties of the reaction centre and of the extent to which the electron is localised within the dimer.

Experimental

Photosystem I particles were prepared from spinach using the non-ionic detergent Triton X-100 as described previously [12]. Samples were prepared at 0.5–4.0 mg chlorophyll per ml in standard 3 mm silica EPR tubes. Comparative measurements were also made on samples prepared with digitonin [13]. Reaction centres from wild type *Rb. sphaeroides* and *R. viridis* were prepared by standard procedures using lauryldiethylamine *N*-oxide as detergent [14,15], samples contained approx. 100 μM reaction centres. P^+ was generated by illumination at room temperature in the EPR tube and freezing in liquid nitrogen under illumination.

Spectra were recorded on a Bruker ESP380 X-band pulsed spectrometer which was equipped with a variable, Q, dielectric resonator (Bruker model 1052 DLQ-H 8907). The sample was maintained at 4 K by an Oxford Instruments, CF935 flowing gas cryostat. For a 16 ns pulse in a $S = 1/2$, $g_e = 2.002$ system, the maximum microwave magnetic field (generated by a 1 kW travelling wave tube amplifier) was approx. 6 G within the 10 mm homogeneous region of the resonator.

All ESEEM spectra were accumulated with a cavity Q of about 100 resulting in a minimum deadtime of approx. 100 ns. A two-pulse, *p-τ-2p-τ-echo* sequence generated a primary ESEEM spectrum where τ the interpulse time is varied, whilst a three-pulse, *p-τ-p-T-p-τ-echo*, phase cycled [16] sequence generated a stimulated ESEEM spectrum where τ is set and T varied. The pulse width, p, was 16 ns (giving a $\pi/2$ (p) or a π ($2p$), tip angle) and in each case the echo was detected with a sampling digitizer. For stimulated ESEEM experiments, τ was fixed at a value between 112 to 456 ns. A typical sweep of T comprised 1024 points with an 8 ns increment and an initial value of 24 ns. There were 20–60 accumulations at every time point and the pulse sequence was repeated at intervals in the range 20–75 ms, depending on the relaxation properties of the species. There were 512 points in a primary ESEEM spectrum, τ being incremented in 8 ns steps whilst other parameters were similar to those used in the stimulated ESEEM experiments.

Before Fourier transform (FT), the echo decay was factored out by subtraction of a polynomial function, high-frequency noise reduced with a fifth-order polynomial filter function and the data set zero filled to increase FT resolution. Spectra are displayed in the power mode (i.e., $real^2 + imag^2$), which eliminates phase problems due to the deadtime but distorts FT amplitude and tends to emphasize minor intensity variations.

A simulation/fitting programme based on Mims' density matrix protocol [17] was written in order to analyze the ^{14}N modulations for these disordered $S = 1/2$, $I = 1$, isotropic g systems.

The interaction of a paramagnetic nucleus with an $S = \frac{1}{2}$ electron spin results in the nucleus being subjected to one of two effective magnetic fields from the vector summation of the applied field and hyperfine

fields from each electron spin orientation such that

$$\nu_{ef}^{-} = |\nu_i - |a_{iso}|/2| \nu_{ef}^{+} = |\nu_i + |a_{iso}|/2|$$

where ν_i is the nuclear Zeeman frequency and a_{iso} is the isotropic hyperfine coupling constant. For systems with $I \geq 1$, such as ^{14}N where $I = 1$, the nucleus has an electric quadrupole moment which interacts with the electric field gradient (EFG). The principal values of the EFG are $V_{xx} \equiv eq_{xx}$, $V_{yy} \equiv eq_{yy}$, $V_{zz} \equiv eq_{zz}$ with principal axes chosen such that $|q_{xx}| \leq |q_{yy}| \leq |q_{zz}|$. The quadrupolar Hamiltonian, H_Q, for the ^{14}N nucleus, $I = 1$, may be written as

$$H_Q = e^2qQ/4\left[3I_z^2 + I^2 + \eta\left(I_x^2 + I_y^2\right)\right]$$

where Q is the scalar quadrupole moment, $q \equiv q_{zz}$, and the asymmetry parameter, η, is defined as

$$\eta = |(q_{xx} - q_{yy})/q_{zz}|$$

The Hamiltonian matrix was factored into 3×3 units, one for each electron spin manifold. Terms included were isotropic hyperfine (a_{iso}), anisotropic hyperfine, modelled by the dipole-dipole approximation (involving r_{eff}, an effective electron nuclear distance), and quadrupole which involves the e^2qQ and η parameters. The spherical model [18] was used to approximate for the multinuclear nature of the chlorophyll cations. Input parameters were a_{iso}, r_{eff}, e^2qQ, η, ϕ, χ (the latter being the Euler angles which allow for non-alignment of the hyperfine and quadrupolar tensors), B_0 (the static magnetic field), ν_M (microwave frequency) and N (the number of equivalent nuclei). Often r_{eff} was set to a constant, 0.35 nm and η, ϕ and χ are set to zero to simplify analysis. Further details can be found elsewhere [18–22].

For these $S = 1/2$, $I = 1$ systems, a characteristic four-line pattern is seen if the applied and hyperfine fields at the nucleus almost cancel or, in other words, if $\nu_{eff} = \nu_i \times a_{iso}/2$ is approximately zero (where ν_i is the nuclear Zeeman frequency). If this 'exact cancellation' condition is met, the lowest two frequencies, ν_0, ν_-, should add up to the third, ν_+, the frequencies being essentially pure nuclear quadrupole resonances (NQR).

$$\nu_0 + \nu_- = \nu_+$$

$$\nu_\pm = (3/4)e^2qQ(1 \pm \eta/3)$$

$$\nu_0 = \tfrac{1}{2}e^2qQ\eta$$

These peaks are usually quite narrow, often similar in intensity and lead directly to estimates of the quadrupole parameters [19]. A double quantum transition, ν_{dq}, in the $\nu_{eff} = \nu_i + a_{iso}/2$ electron manifold, generates the fourth frequency, which can help in estimating a_{iso} [19] as

$$\nu_{dq}^{\pm} = 2\left[|\nu_i \pm |a_{iso}|/2|^2 + \left\{e^2qQ(3+\eta^2)^{\frac{1}{2}}/4\right\}^2\right]^{1/2}$$

However, this transition is often broader and sometimes difficult to distinguish from the background noise.

Results

Analysis of ^{14}N modulation patterns in chlorophylls

As discussed earlier, the NQR peaks are usually quite narrow, often similar in intensity and lead directly to estimates of the quadrupole parameters [19]. The maximum number of transitions observed for a single ^{14}N nucleus coupled to an electron spin is four. If the electron is coupled to more than one nucleus with the same NQR parameters then harmonic and combination frequencies also occur. In the chlorophyll systems studied here, the maximum number of different nitrogen nuclei is eight (four for each chlorophyll in a dimer) and the number of observable frequencies that can be used to accurately determine a_{iso} values is at most 32 (24 NQR plus 8 ν_{dq}). Some simplifying observations are needed to analyze the data.

A useful starting point in the analysis of the modulation spectra is a knowledge of the effects of varying the parameters required to determine the modulation patterns, e^2qQ, η, r_{eff} and a_{iso}. The parameters e^2qQ and η are not expected to greatly influence the spectra as

TABLE I

Comparison of hyperfine and quadrupole parameters derived from ESEEM studies of bacterial and higher plant chlorophyll cations

n.a. = not available.

Species	e^2qQ/(MHz)	η	a_{iso}/(MHz)
P700 [a]	2.72	0.73	2.38
	2.97	0.78	2.23
P870 [a]	2.73	0.66	1.90
P960 [a]	2.90	0.70	2.00
P860 [b]	1.68	0.68	–
	2.72	0.66	–
Chl*a* [c]	2.68	0.60	3.18
	3.20	0.50	2.95
BChl*a* [d]	2.72	0.70	2.35 [e]
	2.80	0.79	3.10 [e]
BChl*b* [d]	n.a.	n.a.	2.30 [e]
	n.a.	n.a.	3.15 [e]

[a] This work.
[b] Ref. 23.
[c] Ref. 24, the values for a_{iso} do not corresspond to a particular set of quadrupole parameters but are estimates based on one double quantum frequency and so only one is correct.
[d] Ref. 35.
[e] The values for a_{iso} were obtained by averaging the reported ^{14}N ENDOR results [27], and do not correspond to a particular set of quadrupole parameters.

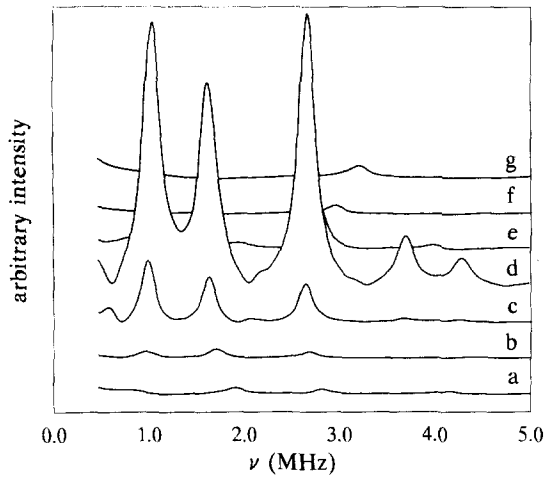

Fig. 1. Simulated FT ESEEM spectra to show the effect of a_{iso}. Parameters, $e^2qQ = 2.84$, $\eta = 0.70$, $\tau = 144$ ns, $\nu_M = 9.76$ GHz, $B_0 \approx 3477.0$ G. a_{iso} = (a) 1.0 MHz, (b) 1.5 MHz, (c) 2.0 MHz, (d) 2.5 MHz, (e) 3.0 MHz, (f) 3.5MHz and (g) 4.0 MHz (note the simulated modulations have been multiplied by an exponential decay curve).

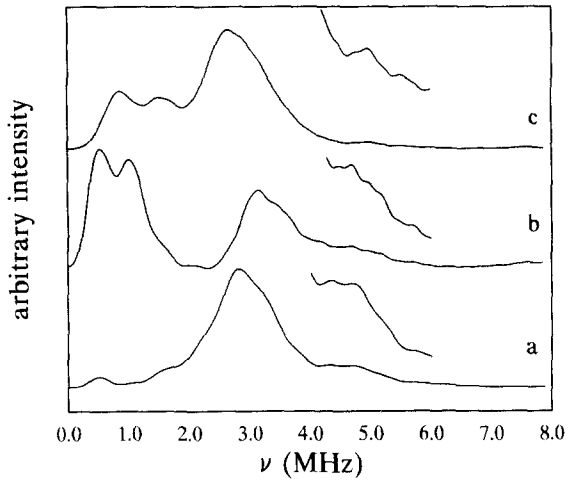

Fig. 2. Primary FT ESEEM spectra of (a) $P870^+$, insert is ×3.5 (b) $P960^+$, insert is ×3.5 (c) $P700^+$, inset is ×8. $\nu_M = 9.76$ GHz, $B_0 = 3477.0$ G. Time domain spectra consisted of 512 points with τ incremented in 8 ns intervals.

the values for these parameters are expected to be similar for all nitrogens in a chlorin ring of a chlorophyll cation. Indeed, ESEEM studies on Chl_a and $BChl_a$ frozen solutions reveal two kinds of nitrogen nuclei with similar quadrupole parameters, approx. e^2qQ values of 2.7 and 3.2 MHz for Chl_a and 2.7 and 2.8 for $BChl_a$, Table I. The effect of a_{iso} is greater, see Fig. 1, in that the although the frequencies of the resonances are not dramatically altered, the relative intensities vary greatly such that for large, ≥ 4 MHz, values of a_{iso} only one frequency is observed in the 0 to 5 MHz range. For nitrogens in a chlorophyll, with $a_{iso} = 1$–4 MHz, the most intense modulation is obtained for approx. $a_{iso} = 2.5$ MHz.

In photosynthetic reaction centres, it is also possible that the electron spin density of the chlorophyll cation is shared between the rings of the chlorophyll dimer. The parameter a_{iso} is proportional to the electron spin density at the nitrogen and is a measure of the extent to which the electron of the chlorophyll cation is shared. Three situations can be envisaged, first electron spin density localized on one of the pair of chlorophylls, (a_{iso} similar to the monomer value), second, equal sharing (a_{iso} approx. half the monomer value), and third an asymmetry in electron spin density over two chlorophylls, (intermediate values of a_{iso}).

$P700^+$, $P870^+$ and $P960^+$

The FT power primary ESE spectra for $P700^+$, $P870^+$ and $P960^+$ are shown in Fig. 2. All the ESEEM spectra are complex with many frequencies observed clustered around three values, 0.8–1.0, 1.5–1.7 and 2.6–3.2 MHz. Figs. 3, 4 and 5 show the FT power stimulated ESEEM patterns of each sample recorded for several different τ values. The use of different τ is required as partial suppression of frequencies can occur at certain values of τ. The use of different τ values also allows for the monitoring of changes in intensity with τ which is useful in the determining of 'real' frequencies as opposed to transform artifacts.

The spectra show more resonances than expected for nitrogens with a single set of parameters. The large number of resonances most likely arises from the presence of nitrogen in more than two kinds of environment with different parameters. Previous studies of reaction center chlorophyll cations have revealed nitrogens with several different a_{iso} values depending on the nature of the experiment, e.g., solution versus frozen glass; Table I.

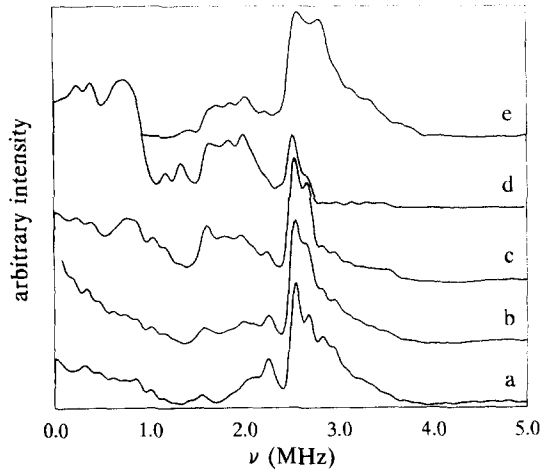

Fig. 3. $P870^+$ (*Rb. sphaeroides*) FT power spectrum of stimulated ESEEM data recorded at several τ. Time domain spectra consisted of 1024 points with an 8 ns increment, $T_{init} = 24$ ns, 40–60 accumulations per point and a repetition time of 20 ms. $\nu_M = 9.758458$ GHz, $B_0 = 3476.7$ G. τ = (a) 112 ns, (b) 136 ns, (c) 168 ns, (d) 200 ns and (e) 264 ns.

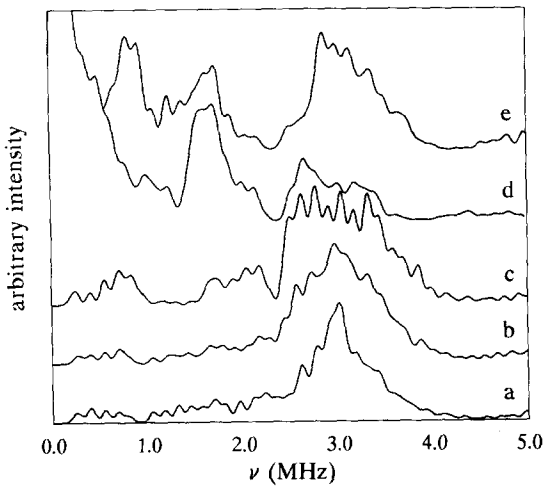

Fig. 4. $P960^+$ (*R. viridis*) FT power spectrum of stimulated ESEEM data recorded at several τ. Time domain spectra consisted of 1024 points with an 8 ns increment, T_{init} = 24 ns, 20–30 accumulations per point and a repetition time of 50 ms. ν_M = 9.765350 GHz, B_0 = 3478.4 G. τ = (a) 112 ns, (b) 136 ns, (c) 168 ns, (d) 200 ns and (e) 264 ns.

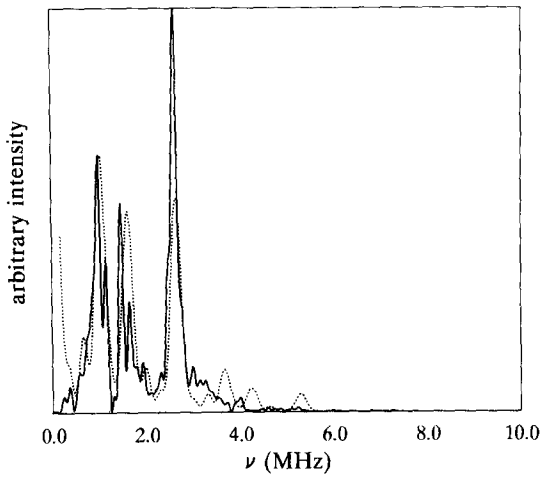

Fig. 6. Simulation of $P700^+$ with τ = 144 ns, ν_M = 9.758849 GHz, B_0 = 3475.7 G, a_{iso} = 2.305 MHz, e^2qQ = 2.81 MHz, η = 0.75, r_{eff} = 0.35 nm, N = 4. Experimental trace (———), simulated trace (-----). Time domain data consisted of 512 points incrementing at 16 ns with T_{init} = 24 ns. 2025 time domain data sets were averaged over a half sphere to approximate a powder spectrum. Modulations in domain damped by multiplying with an exponential of time constant 2.0 μs.

$P870^+$ and $P960^+$

Frequencies at 0.8, 1.6, and 2.5 MHz for $P870^+$ lead to e^2qQ = 2.73 MHz and η = 0.66 whilst adopting the procedure of Dikanov et al. [23] the boundary condition $3.9 < \nu_{dq} < 6.2$ MHz suggests that $\nu_{dq} \approx 4.8$ MHz (see Fig. 2) and therefore a_{iso} = 1.9 MHz.

The $P960^+$ spectra have a broad range of frequencies centred on 3 MHz. The frequencies 0.8, 1.7 and 2.7 MHz appear to belong to a set. This leads to e^2qQ = 2.9 MHz, η = 0.7, $\nu_{dq} \approx 5.0$ MHz (see Fig. 2) and $a_{iso} \approx 2.0$ MHz which can be compared to an average ENDOR value of 2.5 MHz. [24]

De Groot et al. [25] obtained two sets of quadrupole parameters for their ESE study of *R. rubrum* $P870^+$, namely e^2qQ = 1.68, 2.72 MHz and η = 0.68, 0.66. There appear to be two or more sets in *R. sphaeroides* $P870^+$ and *R. viridis* $P960^+$, however, the complexity of the spectra, combined with the lack of resolution, confounds attempts to define more than one set. It appears from the spectra of De Groot et al. [25] that complexity (and hence apparent breadth) decreases with increase in τ as some of the frequencies are lost as they damp out. Simulations were attempted for both the bacterial primary donors but met with limited success, because the extra line breadths, related to the damping, thwarted efforts to extract more than one set of molecular parameters. By multiplying the simulations according to their experimental modulation decay time, a broadening effect was obvious, but could not account for the full linewidth. In these bacterial reaction centres a non-haem iron is located close, 27.9Å, to the primary chlorophylls, while *R. viridis* additionally has a four-haem cytochrome as the electron donor with closest iron centre at 20.5Å. These iron centres probably act to cause the damping.

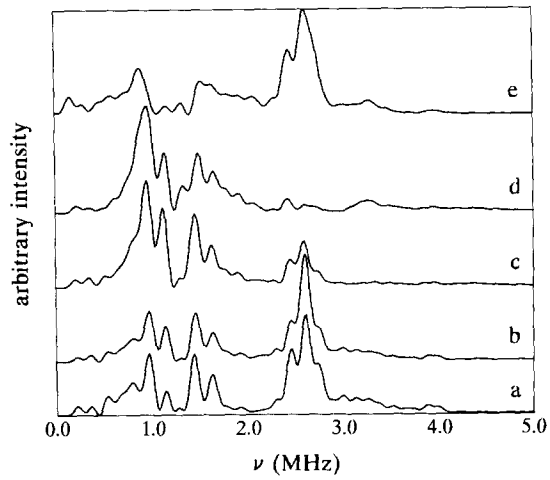

Fig. 5. $P700^+$ FT power spectrum of stimulated ESEEM data recorded at several τ. Time domain spectra consisted of 1536 points with an 8 ns increment, T_{init} = 24 ns, 20 accumulations per point and a repetition time of 40 ms. ν_M = 9.753917 GHz, B_0 = 3476.5 G. τ = (a) 112 ns, (b) 136 ns, (c) 168 ns, (d) 200 ns and (e) 264 ns.

$P700^+$

In $P700^+$, there are five main frequencies: at 0.98, 1.14, 1.45, 1.64 and 2.63 MHz. From these five frequencies it is possible to form two sets that fulfil the exact cancellation condition. First with 0.98, 1.64 and 2.63 MHz, the other with 1.14, 1.45 and 2.63 MHz. Since ν_i is about 1.07 MHz at 3476 G for ^{14}N, a_{iso} must be around 2 MHz [23]. It is possible to predict the following bounds for ν_{dq}, $3.88 < \nu_{dq} < 6.20$ MHz. The likely candidate can be seen most easily in the primary ESEEM spectrum at 5.27 MHz (see Fig. 2), which

leads to a_{iso} values of 2.32 and 2.35 MHz respectively. A combination of simulations and further use of the equations for the NQR frequencies [19] yields e^2qQ = 2.84, and 2.69 MHz with $\eta = 0.70$ and 0.85. These values are comparable to Dikanov's estimates of e^2qQ = 2.6 MHz, $\eta = 1$ and $a_{iso} = 2.24$ MHz [23] and in a more recent report $e^2qQ = 2.76$ MHz and $\eta = 0.76$ [26].

Fits to the data have been attempted in which the molecular constants and number of classes of nuclei were varied using the above estimates as an initial basis in order to ascertain the appropriateness of the values. Unfortunately, we were unable to obtain a unique fit with two sets of input parameters. However, the fit with one set of parameters, Fig. 6, resulted in an a_{iso} value which agrees with the average value estimated from the double quantum frequency as well as broadly predicting the intensity variation as τ is increased (not shown.)

EPR, ENDOR, TRIPLE and molecular orbital studies have generated worthwhile theoretical and experimental data on $P870^+$ and $P960^+$ [24,27–33], and there have been ESEEM studies of both ^{14}N [23] and ^{15}N [34] $P860^+$ in *R. rubrum*, a species which should be structurally similar to *R. sphaeroides* and *R. viridis.*

Table I compares e^2qQ, η and a_{iso} values from this and other ^{14}N ESEEM studies for various chlorophyll cations.

Discussion

The ESEEM spectrum of $P700^+$ has previously been recorded at 77 K by Dikanov et al. [23] but contained fewer frequencies compared to the 4 K data presented here. The paucity of frequencies in Dikanov's high temperature spectrum is probably due to the decay of some of the components within the longer spectrometer deadtime, coupled with the decrease in the phase memory time at the higher temperature.

The current work has yielded values for hyperfine (a_{iso}) and quadrupole (e^2qQ and η) parameters in $P870^+$, $P960^+$ and $P700^+$. For each of these chlorophylls there is evidence that more than two sets of parameters are required to simulate the spectra. The major features of the $P700^+$ spectra were simulated. Simulations of the bacterial signals, although limited in success, proved that the linewidths could not be accounted for solely on the basis of the spectrometer deadtime. It would be interesting to obtain data on bacterial systems which have the non-haem iron removed, as a means of increasing the phase memory time, to obtain better estimates of a_{iso}.

Comparison of quadrupole parameters in bacterial, higher plant and isolated chlorophyll cations (Table I) reveals that they are similar in all species. This is to some extent expected, since they are a reflection of contributions from all the electrons [35]. The a_{iso} values (derived from ENDOR and ESEEM) are a more sensitive probe of electron density and in the dimeric bacterial primary donor systems are smaller than for isolated chlorophylls which reflects the monomeric nature of the latter. Previous studies on the bacterial reaction centres has revealed differences in the distribution of the electron spin density, as measured by a_{iso}, between the chlorophylls of the special pair dimer. In the case of $P870^+$, initial studies indicated the electron to be 'shared' (1 : 1) by the two chlorophylls of the dimer, while for $P960^+$, a degree of localisation was thought to occur (2 : 1). A more recent study of $P870^+$ has estimated the distribution of electron spin density over the chlorophyll dimer to be 2 : 1, as in $P960^+$. [5].

An estimate of the electron spin density distribution within the special pair chlorophyll cation can be obtained from the ratio of the measure a_{iso} from the reaction centre chlorophyll cation to that of the monomeric chlorophyll cation, $a^{rc}{}_{iso}/a^{mon}{}_{iso}$. As discussed earlier, the ESEEM spectra are dominated by the nitrogens with a_{iso} close to 2.5 MHz, which is close to the largest a_{iso} observed for the monomeric chlorophylls listed in Table I, the range observed in ENDOR/TRIPLE and theoretical studies for a_{iso} is 0.61–2.71 MHz. We expect to select the frequencies related to the nitrogen with the largest a_{iso} observed in monomeric chlorophll. If the electron is delocalised over a dimer then the values of a_{iso} are reduced, and the measured ESEEM a_{iso} value once more relates to the nitrogen with the largest a_{iso}, i.e., we expect to select the frequencies associated with the largest a_{iso} value in the dimeric system. If the electron was equally distributed over both chlorophyll molecules the maximum value of a_{iso} would be 1.30 MHz. The experimental estimate should therefore be compared with the largest of the a_{iso} values for the monomeric chlorophyll. The data suggest the distribution of electron spin density is the same for $P870^+$, $a^{rc}{}_{iso}/a^{mon}{}_{iso}$ approx. $1.9/3.3 = 0.6$ (2 : 1) and $P960^+$ $a^{rc}{}_{iso}a^{mon}{}_{iso}$ approx. $2.0/3.3 = 0.6$ (2 : 1).

The reduction in the a_{iso} for $P700^+$ compared to in vitro studies of Chl_a^+ could also arise from either a modified chlorophyll monomer, e.g. Chl_a covalently bound to the protein matrix or derivatised, or from a Chl_a dimer. However, modified Chl_a monomers, enol and chlorinated derivatives as well as Chl_a monomers covalently bonded to the protein are considered less likely as improved extraction methods and analysis of the vibrational spectra of the chlorophylls have failed to find evidence for modified chlorophylls. Assuming that the primary donor is a Chl_a dimer, the values of the a_{iso} for $P700^+$ are once more indicative of an asymmetric distribution of electron spin density, $a^{rc}{}_{iso}/a^{mon}{}_{iso}$ approx. $2.3/3.2 = 0.75$ (3 : 1) or $2.3/2.95$

= 0.78 (4 : 1), depending on which of the Chl_a monomer estimates are correct (see Table I).

The decay of the modulations can also reveal information about the magnetic environments of the primary donors if we again assume that the electron couplings are similar for these chlorophylls studied. Damping of the modulations occurred in the order $P960^+ > P870^+ > P700^+$. The structure of the bacterial reaction centres includes a non-haem iron 27.9Å from the primary donor and in $P960^+$ a donor cytochrome, cyt *c*, which is approx. 20.5 Å from the primary donor. In Photosystem I the redox centres which may contribute to damping of the modulations are the bound iron-sulphur centres. Comparisons of the modulation damping for bacterial systems and $P700^+$ with $Fe\text{-}S^-_{A/B}$ reduced and oxidised, suggests that the iron-sulphur centres in PS-1 are further away from the primary donor in PS-1 compared to the iron centres in bacterial reaction centres, consistent with the cofactors expected location on opposite sides of the membrane. We are currently investigating the effect of $Fe\text{-}S^-_X$ on the $P700^+$ spin echo.

Future work will involve comparison with other known monomers, dimers and model compounds at different microwave frequencies.

Acknowledgments

This work was supported by grants from the UK Science and Engineering Research Council and University of London Intercollegiate Research Service.

References

1 Norris, J.R. and Katz, J.J. (1978) in The Photosynthetic Bacteria (Clayton, R.K. and Sistrom, W.R., eds.), pp. 397–418, Plenum Press, New York.
2 Feher, G., Hoff, A.J., Isaacson, R.A., Ackerson, C.C., (1975) Ann. N.Y. Acad. Sci. 244, 239–259.
3 Budil, D.E. and Thurnauer, M.C. (1991) Biochim. Biophys. Acta 1057, 1–41.
4 Deisenhofer, J. and Michel, H. (1991) Annu. Rev. Biophys. Biophys. Chem. 20, 247–266,
5 Feher, G. (1993) R. Soc. Chem. Bruker Lecture, J. Chem. Soc. Faraday Trans., in press.
6 Moenne-Loccoz, P., Robert, B., Ikegami, I. and Lutz, M. (1990), Biochemistry 29, 4740–4746.
7 Karapetyan, N.V., Shubin, V.V., Rakhimberdieva, M.G., Vashchenko, R.G. and Bolychevtseva, Y.V. (1984) FEBS Lett. 173, 209–212.
8 Itoh, S., Iwaki, M. and Ikegami, I. (1981) Biochim. Biophys. Acta 893, 508–516.
9 Norris, J.R., Uphaus, R.A., Crespi, H.L. and Katz, J.J. (1971) Proc. Natl. Acad. Sci. USA 68, 625–629.
10 Norris, J.R., Scheer, H., Druyan, M.E. and Katz, J.J. (1974) Proc. Natl. Acad. Sci. 71, 4897–4900.
11 O'Malley, P.J. and Babcock, G.T. (1984) Proc. Natl. Acad. Sci. USA 81, 1098–1101.
12 Williams-Smith, D.L., Heathcote, P., Sihra, C.K. and Evans, M.C.W (1978) Biochem. J. 170, 365–372.
13 Boardman, N.K. (1971) Methods Enzymol. 23, 268–276.
14 Clayton, R.K. and Clayton, B.J. (1978) Biochim. Biophys. Acta 501, 470–477.
15 Jolchine, G. and Reiss-Husson, F. (1974) FEBS Lett. 40, 5–8.
16 Fauth, J.-M., Schweiger,A., Forrer, J. and Ernst, R.R. (1986) J. Mag. Res. 66, 74–85.
17 Mims, W.B. and Peisach, J.(1978) J. Chem. Phys. 69, 4921–4930.
18 Heming, M., Narayana, M. and Kevan, L. (1985) J. Chem. Phys. 83, 1478–1484.
19 Britt, R.D., Zimmermann, J.L., Sauer, K. and Klein, M.P. (1989) J. Am. Chem. Soc. 111, 3522–3536.
20 Bowman, M.K. and Massoth, R.J. (1987) in Electronic Magnetic Resonance of the Solid State (Weil, J.M., ed.), pp. 99–110, Canadian Society of Chemistry, Ottawa
21 Tsvetkov, Y.D. and Dikanov, S.A. (1981) in Metal Ions in Biological Systems (Helmut, S., ed.), Ch. 5, pp. 207–263.
22 Muha, G.M. (1980) J. Chem. Phys 73, 4139–4140.
23 Dikanov, S.A., Astashkin, A.V., Tsvetkov, Yu.D. and Goldfeld, M.G. (1983) Chem. Phys. Lett. 101, 206–210.
24 Lendzian, F., Lubitz, W., Scheer, H., Hoff, A.J., Plato, M., Tränkle, E. and Möbius, K. (1988) Chem. Phys. Lett. 148, 377–385.
25 De Groot, A., Hoff, A.J., De Beer, R. and Scheer, H. (1985) Chem. Phys. Lett. 113, 286–290.
26 Dikanov, S.A. and Astashkin, A.V. (1990) in Advanced EPR in Biology and Biochemistry (Hoff, A.J., ed.), Ch. 2, pp. 59–117, Elsevier Amsterdam.
27 Lendzian, F., Lubitz, W., Steiner, R., Tränkle, E., Plato, M., Scheer H. and Möbius, K. (1986) Chem. Phys. Lett. 126, 290–296.
28 Plato, M., Lubitz, W., Lendzian F. and Möbius, K. (1988) Isr. J. Chem. 28, 109–119.
29 Petke, J.D., Maggiora, G.M., Shipman, L.L. and Christoffersen, R.E. (1980) Photochem. Photobiol. 36, 243–257.
30 Huber, M., Lendzian, F., Lubitz, W., Trankle, E., Mobius, K. and Wasielewski, M.R. (1986) Chem. Phys. Lett. 132, 467.
31 Möbius, K., Plato, M., Lubitz, W. and Lendzian, F. (1988) Isr. J. Chem 28, 239–248.
32 Astashkin, A.V., Dikanov, S.A. and Tsvetkov, Yu.D. (1988) Chem. Phys. Lett. 152, 258–264.
33 Plato, M., Lendzian, F., Lubitz, W., Tränkle, E. and Möbius, K. (1988) NATO ASI Ser. Ser. A, Photosnth. Bact. React. Cent. 1, 149, 379–388.
34 Lin, C.P., Bowman, M.K. and Norris, J.R. (1986) J. Chem. Phys. 85, 56–62.
35 Hoff, A.J., De Groot, A., Dikanov, S.A., Astashkin, A.V. and Tsvetkov, Yu.D. (1985) Chem. Phys. Lett. 118, 40–47.